PAPER

pH and concentration dependence of the optical properties of thiol-capped CdTe nanocrystals in water and D$_2$O†

R. Schneider,[ab] F. Weigert,[a] V. Lesnyak,[c] S. Leubner,[c] T. Lorenz,[d] T. Behnke,[a] A. Dubavik,[e] J.-O. Joswig,[d] U. Resch-Genger,*[a] N. Gaponik[c] and A. Eychmüller[c]

The optical properties of semiconductor nanocrystals (SC NCs) are largely controlled by their size and surface chemistry, *i.e.*, the chemical composition and thickness of inorganic passivation shells and the chemical nature and number of surface ligands as well as the strength of their bonds to surface atoms. The latter is particularly important for CdTe NCs, which – together with alloyed Cd$_x$Hg$_{1-x}$Te – are the only SC NCs that can be prepared in water in high quality without the need for an additional inorganic passivation shell. Aiming at a better understanding of the role of stabilizing ligands for the control of the application-relevant fluorescence features of SC NCs, we assessed the influence of two of the most commonly used monodentate thiol ligands, thioglycolic acid (TGA) and mercaptopropionic acid (MPA), on the colloidal stability, photoluminescence (PL) quantum yield (QY), and PL decay behavior of a set of CdTe NC colloids. As an indirect measure for the strength of the coordinative bond of the ligands to SC NC surface atoms, the influence of the pH (pD) and the concentration on the PL properties of these colloids was examined in water and D$_2$O and compared to the results from previous dilution studies with a set of thiol-capped Cd$_{1-x}$Hg$_x$Te SC NCs in D$_2$O. As a prerequisite for these studies, the number of surface ligands was determined photometrically at different steps of purification after SC NC synthesis with Ellman's test. Our results demonstrate ligand control of the pH-dependent PL of these SC NCs, with MPA-stabilized CdTe NCs being less prone to luminescence quenching than TGA-capped ones. For both types of CdTe colloids, ligand desorption is more pronounced in H$_2$O compared to D$_2$O, underlining also the role of hydrogen bonding and solvent molecules.

Introduction

In the last decades, colloidal semiconductor nanocrystals (SC NCs) have matured from objects and tools of basic research to a class of photoluminescent materials increasingly employed in life and material sciences, optical technologies, and telecommunication. Typical applications range from fluorescent reporters in bioimaging studies, immunohistochemistry, and fluorescence assays to active materials in solar cells, displays, and solid state lighting.[1–3] High quality SC NCs present sophisticated core–shell or core-only architectures covered with organic surface ligands that are bound to surface atoms either coordinatively or electrostatically or interact with them *via* van der Waals forces.[4] The type and amount of ligands control not only particle nucleation and growth during synthesis, thereby determining particle core formation, its size and size distribution, yet it also determines SC NC solubility in different media and the choice of suitable conjugation chemistries for subsequent (bio)-functionalization. More important, they have a strong impact on the photoluminescence (PL) properties, *i.e.*, the value of the PL quantum yield (PL QY), and partly also on the PL decay kinetics of SC NCs.[5] This is related to the passivation of surface defects, *i.e.*, incompletely coordinated metal or chalcogen atoms on the SC NC surface, which eliminates or strongly reduces nonradiative charge trapping decay pathways of optically generated excitons. Hence, the value of the PL QY and the PL decay behavior reflect directly the surface coverage of such NCs.[6–8]

Suitable surface passivation of SC NCs requires a sufficient change in the energetic position of localized trap states for optimum results. In addition, surface ligands can also affect the degree of quantum confinement and can exchange charge

[a] Federal Institute for Materials Research and Testing (BAM), Richard-Willstätter-Str. 11, 12489 Berlin, Germany. E-mail: ute.resch@bam.de

[b] Institute of Chemistry, University Potsdam, Karl-Liebknecht-Straße 24-25, 14476 Potsdam-Golm, Germany

[c] Physical Chemistry and Center for Advancing Electronics Dresden, TU Dresden, Bergstr. 66b, 01062 Dresden, Germany

[d] Theoretical Chemistry, TU Dresden, Bergstr. 66b, 01062 Dresden, Germany

[e] ITMO University, 197101 Saint Petersburg, Russia

† Electronic supplementary information (ESI) available. See DOI: 10.1039/c6cp03123d

This journal is © the Owner Societies 2016

Phys. Chem. Chem. Phys., 2016, **18**, 19083–19092 | 19083

carriers with photoexcited SC NCs, depending on the energies of their highest occupied (HOMO) and lowest unoccupied (LUMO) molecular orbitals.[9] This underlines the high importance of the strength of the SC NC surface atom–ligand bond for their optical properties, especially for all measurements and applications, where the initial SC NC concentration and/or the SC NC micro-environment are changed. Other factors to be considered include the number of functional groups, ligand size, and the electronic nature of the ligand–surface atom bond as well as the possible removal of surface ligands by protonation of their metal coordinating sites and hence, the ligand's (de)protonation constant (K_a).[10,11] This can introduce a pH dependence of the optical properties and the colloidal stability. Moreover, the dielectric constant of the ligand layer can affect SC NC PL. Also, with the aid of properly chosen surface ligands, blinking of SC NC can be suppressed or reduced[12] and only recently, it was shown that the PL QY of SC NCs can be restored upon addition of extra surface ligands.[13]

The influence of ligand–surface interactions on the optical properties of SC NCs is not yet fully understood despite of their importance for many applications of SC NCs and their development into routinely used fluorescent tools. Such interactions are also influenced by size- and material-specific effects including the chemical composition of the SC NC material and more importantly, its surface, as well as the chemical nature of the ligands.[8,14] This further complicates the already complex interplay of multiple parameters.

A better understanding of ligand–surface interactions requires simple methods for the determination of the number of surface ligands per SC NC and the shell structure, as was recently shown by us for CdTe colloids synthesized with different shell structures by means of simple tests of the quality of the ligand shell.[15,16] Moreover, the rational design of highly emissive SC NCs calls for systematic and really comparable studies on the influence of commonly used surface ligands like short chain mono or bidentate thiols with charged end groups on their optical properties and the influence of pH on SC NC stability and PL. For example, recent studies of the pH dependence of the PL of CdTe NCs capped with thiol ligands like thioglycolic acid (TGA), mercaptopropionic acid (MPA), hydroxyl-terminated 1-thioglycerol (TG), and amine-terminated 1-thioglycerol (MA) revealed a complex correlation between the terminal group of the ligand engaged in free ligand–Cd^{2+} complexes and secondary coordination, SC NC aggregation induced by protonation of electrostatically stabilizing charged ligands, thiol protonation, and the influence of counter ions.[17] Such studies are also important for ligand design, which is being increasingly used e.g., for better control of the nano–bio interface.[18–21]

Aiming at a deeper understanding of the role of surface ligands, we address here the question how the type and the amount of monodentate thiol surface ligand, pH, and hydrogen bonding as well as SC NC concentration influence the colloidal stability and the PL features of CdTe NC colloids. In this respect, a set of TGA- and MPA-stabilized CdTe SC NCs of representative size was prepared following established methods[22–24] and analytically characterized regarding the number of surface ligands per SC NC. Subsequently, their optical properties and colloidal

stability were assessed as a function of pH and dilution/SC NC concentration in water as well as in D$_2$O. D$_2$O, used e.g., for NMR studies of the ligand shell of SC NCs[25–30] was chosen as a solvent for the characterization of the surface composition of SC NCs in order to assess the influence of hydrogen bonding. We focus here on steady state PL measurements, PL dynamics, and the correlation of the observed changes to obtain information on quenching effects associated with e.g., ligand desorption. Moreover, the results were compared with previously performed studies of ternary CdHgTe SC NCs stabilized with different monodentate thiol ligands.[14]

Experimental

Materials

All chemicals used were of analytical grade or of the highest purity available and employed as received: Cd(ClO$_4$)$_2$·6H$_2$O (Alfa Aesar), Al$_2$Te$_3$ (Cerac Inc.), NaOH (Aldrich), NaOD (Merck), H$_2$SO$_4$ (Aldrich), DCl (Aldrich), HCl (Aldrich), D$_2$O (Aldrich), TGA (Merck), and MPA (Aldrich). All aqueous solutions were prepared with Milli-Q water (Millipore). The QY standard Nile Red (batch number 333298/1 1196) was obtained from Lambda Physik. Ethanol employed for dissolving of the QY standard was of spectroscopic grade and purchased from Aldrich. For the Ellman's test, 5,5′-dithiobis(2-nitrobenzoic acid) (DTNB, Ellman's reagent) (Aldrich), NaH$_2$PO$_4$ (Aldrich), Na$_2$EDTA (Aldrich), and Na$_3$PO$_4$ (Aldrich) were used.

Synthesis of thiol-capped CdTe NCs

MPA- and TGA-capped CdTe NCs were synthesized according to a previously reported procedure.[22–24] The initial molar ratio of Cd^{2+} : Te^{2-} : thiol was set to 1.00 : 0.75 : 1.30 for all syntheses. Cd(ClO$_4$)$_2$·6H$_2$O was dissolved in 250 mL of ultrapure water in a three-necked flask equipped with valves and septa, and either TGA or MPA was added under stirring. The pH was adjusted to 12 by dropwise addition of a 1 M NaOH solution and oxygen was removed by flushing with argon for 1 h. H$_2$Te gas, generated by reaction of Al$_2$Te$_3$ lumps with 0.5 M H$_2$SO$_4$, was bubbled through the solution for ca. 30 min in a slow argon stream under stirring. Formation and growth of the NCs proceeded upon reflux. All synthetic key parameters such as temperature, initial molar ratio of Cd, Te, and thiol, reaction volume, and pH were kept constant to ensure identical growth conditions. The as prepared CdTe colloids were concentrated on a rotary evaporator. Unless otherwise stated, all SC NC colloids investigated were purified by precipitation of the as synthesized SC NCs with 2-propanol. The precipitated CdTe NCs were subsequently redispersed either in water or D$_2$O. No special post-preparative treatments to control and reduce the size distribution or to increase PL QY were applied.

Methods

Characterization of the CdTe NCs. Samples for transmission electron microscopy (TEM) were prepared by dropping a diluted NC solutions on a copper grid coated with a silicon dioxide film

19084 | *Phys. Chem. Chem. Phys.*, 2016, **18**, 19083–19092

This journal is © the Owner Societies 2016

and subsequently evaporating the solvent. TEM imaging was carried out on a Tecnai F20 microscope (FEI Company), operating at 200 kV acceleration voltage.

Optical spectroscopy. UV/Vis absorption spectra were recorded with a calibrated Cary 5000 spectrophotometer (Varian Inc., Palo Alto, USA). The absorption spectra were used for determination of the size of the colloids from the spectral position of the first excitonic absorption peak with the aid of size curves[23,31,32] and controlled by comparison with the TEM data. Steady state PL measurements were performed with a calibrated FLS-920 fluorometer (Edinburgh Photonics) at BAM, equipped with a Xe lamp, Czerny–Turner double monochromators, a reference channel, and Glan–Thompson polarizers placed in the excitation and emission channels set to 0° and 54.7°, respectively (magic angle conditions) to render detected emission intensities independent of possible emission anisotropies.[33–35] All fluorescence spectra shown were corrected for the wavelength-dependent spectral responsivity of the fluorometer's detection channel as previously reported.[36] The relative determination of PL QY from the absorption spectra and integrated corrected emission spectra (blank and spectral correction; consideration of the photonic nature of the emitted light) of the sample and standard in air-saturated solution was performed according to a previously published protocol.[8] We used the quantum yield standard Nile Red (excitation wavelength: 500 nm; solvent ethanol; PL QY = 0.64).[14,37] PL QY values were calculated from integral spectrally corrected emission spectra (referenced to the spectral photon radiance scale), with consideration of the refractive indices of the solvents used for the SC NCs and the QY standard.[34] All absorption and fluorescence measurements were performed with air-saturated and freshly prepared SC NC dispersions at $T = (25 \pm 1)$ °C using 10 × 10 mm quartz cuvettes from Hellma GmbH if not otherwise stated. The absorbance of the SC NC and dye solutions used for determination of the PL QY was within the range of 0.02 to 0.10 at the excitation wavelength.

Time-resolved fluorescence measurements. Fluorescence decay curves were recorded in 10 × 10 mm quartz cuvettes (Hellma) with a FLS-920 fluorescence lifetime spectrometer (Edinburgh Instruments) equipped with a super-continuum laser (Fianium SC400-2-PP) set to a pulse repetition rate of 1 MHz using time-correlated single-photon counting (TCSPC) without polarizers.[12,23] All samples were excited at 500 nm, while the emission was detected at the emission maximum of each sample employing a spectral bandwidth of the emission monochromator of 12 nm. The calculated lifetimes represent the time after which the initial fluorescence intensity decreased to the $1/e$ part of its maximum value.

Ellman's test. Quantification of the average number of thiol ligands per SC NC was performed with the Ellman's test[38,39] previously validated by us for the analysis of monodentate ligands on SC NCs like TGA.[14,15] A 3.4×10^{-3} M stock solution of DTNB was prepared in 0.1 M phosphate buffer (NaH₂PO₄) containing 1×10^{-3} M EDTA (pH 8.0, adjusted with NaOH). Addition of EDTA led to complete dissolution of the colloid as controlled by absorption and fluorescence measurements. For calibration, a freshly prepared aqueous stock solution of each

ligand (3×10^{-3} M) was used. For this assay, 2900–2949 μL of buffer, 50 μL of Ellman's reagent solution, and 1–50 μL of the sample or calibration solution were mixed. To monitor the reaction process, absorption spectra were recorded in intervals of 10 min until the absorption remained constant. The thiol concentration was determined after complete reaction by comparison of the absorbance at 409 nm with the calibration curve obtained for the pure ligand.

ICP-OES. All measurements were done with diluted SC NC samples without further treatment using a Horiba Jobin Yvon Ultima 2CHR instrument. The wavelengths chosen for quantification were 228.802 nm (Cd), 180.676 nm (S), and 214.281 nm (Te), respectively. All results were obtained from triple measurements. The relative standard deviations were below 3%.

Dilution studies in H₂O and D₂O at different pH/pD. An aqueous and a deuterated phosphate buffer (0.01 M Na₃PO₄) were prepared in H₂O and D₂O and adjusted to five different pH/pD values with HCl/DCl. For each pH/pD value, fresh samples were prepared by dilution of varying amounts (1 to 80 μL) of the concentrated aqueous SC NC stock solution. The concentrations of the SC NC stock solutions were 3.31×10^{-5} (M2), 5.13×10^{-5} (T2), 1.59×10^{-4} (T3), and 3.85×10^{-4} M (M3), respectively, as calculated from the size curves and size-dependent extinction coefficients given by Rogach,[23] Yu,[31] and Ji.[32] The volume of the measurement solutions was 3 mL for 10 × 10 mm conventional optical cells suitable for absorption and fluorescence and 15 mL for 10 × 50 mm cells used solely for absorption measurements of very dilute SC NC solutions with absorbances <0.01 at 500 nm. The pH/pD values were always controlled before and after the measurement of the absorption and emission spectra.

The pD values provided here present the analog of the pH in D₂O solution. These values differ from pH due to the different dissociation constants of H₂O and D₂O. They can be obtained from pH measurements with a glass electrode in D₂O solution according to eqn (1).[40]

$$pD = pH_{reading} + 0.40 \qquad (1)$$

Molecular-dynamics (MD) simulations. The MD simulations were performed using the density-functional tight-binding approach[41–43] in a self-consistent charge extension.[44] The cubic simulation box (a = 0.99 nm) contained 32 H₂O or D₂O molecules, respectively. A 30 ps equilibration phase was followed by a 30 ps production run with a time step of 0.25 fs at 300 K. Snapshots were taken every 10 fs, which were analysed with respect to hydrogen bonds (distance criterion: 0.25 nm) as previously reported.[45,46]

Results and discussion

Surface chemistry and spectroscopic properties of TGA- and MPA-stabilized CdTe SC NC

The CdTe SC NCs were characterized by TEM, ICP-OES, the photometric Ellman's test as well as steady state and time-resolved fluorometry. The absorption and emission spectra are illustrated in Fig. 1 and the relevant analytical and spectroscopic properties
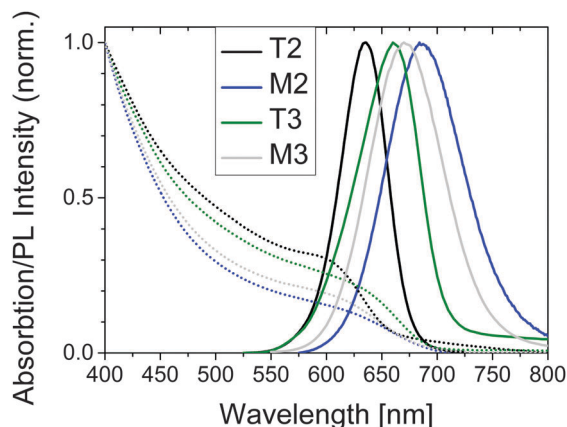
This journal is © the Owner Societies 2016

Phys. Chem. Chem. Phys., 2016, **18**, 19083–19092 | 19085

Fig. 1 Normalized absorption (dotted lines)- and emission spectra (solid lines) of CdTe-TGA NC samples T2 and T3 and CdTe-MPA NC samples M2 and M3 in water (pH 9). Excitation was at 500 nm. The absorption spectra shown present the wavelength dependence of the measured absorbance.

are summarized in Table 1. As follows from these data, the sizes of the TGA- and MPA-stabilized CdTe samples T2 and M2 and T3 and M3 are comparable, typical TEM images are provided in Fig. S1 (in the ESI†). With PL QY values between 41 and 57%, our CdTe NCs reveal the moderate to high PL QYs to be expected for high quality CdTe colloids.

Influence of pH

The PL properties of TGA- and MPA-stabilized CdTe colloids are considerably influenced by pH as shown in Fig. 2 for the colloids T2 and M2, with the type of thiol ligand affecting pH-induced spectral and intensity changes.

In the case of TGA-stabilized CdTe T2, the spectral position and shape of the emission spectra are not affected by pH in the alkaline pH range. As follows from Fig. 2 (top panel), at pH 7.4 and pH 6.6, the lowest pH values where we could still observe luminescence, the luminescence was slightly blue shifted by 2 nm and 4 nm, respectively. This blue shift was also seen in the absorption spectra (Fig. S4, ESI†) and may provide a hint for particle oxidation as result of ligand desorption.[47] No emission was detectable at pH ≤ 6.6.

At pH 4.6, the absorption spectra of TGA-stabilized CdTe show a slight red shift, the absorption starts do decrease, and the dispersion starts to scatter. This suggests protonation-induced
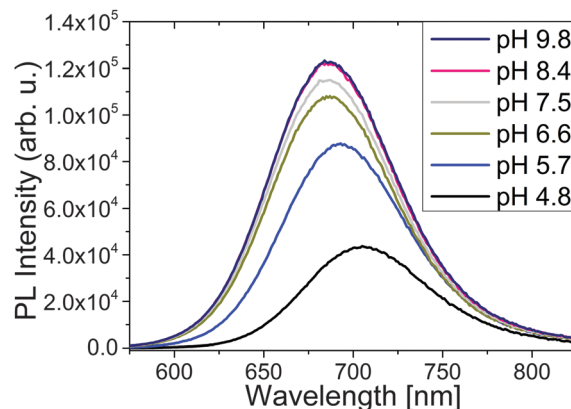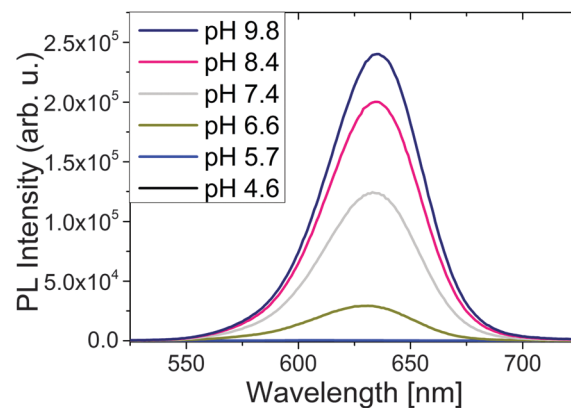

Fig. 2 Emission spectra of TGA-stabilized CdTe T2 (top) and MPA-stabilized CdTe M2 (bottom) at constant concentration and different pH in water. Excitation was at 500 nm.

PL quenching, accompanied by (and maybe also related to) the onset of particle agglomeration.

In contrast, for the MPA-stabilized CdTe sample M2, a reduction in pH is accompanied by a slight decrease in PL intensity for pH values below 8.4. This diminution in PL intensity becomes more pronounced for pH values ≤ 6.6 (Fig. 2, lower panel) and is accompanied by a considerable red shift in emission. The absorption spectra, however, are barely affected by pH in the range of 9.8 to 4.8 (see ESI,† Fig. S4, right panel) and the dispersion remains transparent. The red shift in emission might be due to an increased contribution of PL originated from surface states. Below pH 4.8, also for MPA-stabilized CdTe NCs, an acidic pH induces particle growth and a change in the particle size distribution, yet the particles remain luminescent even at acidic pH values up to 4.8 and are still colloidally stable. At pH values < 4.8, also MPA-capped CdTe NCs aggregate and become nonemissive.

Fig. 3 compares the pH dependence of the TGA- and MPA-stabilized CdTe samples, revealing a diminution in PL QY with decreasing pH for both ligands. While for CdTe-TGA (T2), no emission was detectable at pH ≤ 6.6, the CdTe-MPA sample (M2) was still luminescent at pH 4.8. Moreover, for MPA-stabilized CdTe, the PL QY remained constant above pH 8.4 whereas the PL QY of TGA-capped CdTe steadily increased with increasing pH

Table 1 Characterization of the TGA- and MPA-stabilized CdTe NCs T2, T3, M2 and M3: SC NC sizes obtained from sizing curves (representatively controlled by TEM), spectroscopic properties, and average ligand densities derived from ICP-OES and the Ellman's test

Properties	CdTe-TGA T2	CdTe-TGA T3	CdTe-MPA M2	CdTe-MPA M3
Diameter [nm]	3.3 ± 0.1	3.8 ± 0.1	3.7 ± 0.1	3.5 ± 0.1
First excitonic max. [nm]	600 ± 6	630 ± 6	625 ± 6	610 ± 6
Emission max. [nm]	635 ± 2	663 ± 2	685 ± 2	666 ± 2
FWHM$_{em}$ [nm]	49.6 ± 0.3	56.9 ± 1.2	82.2 ± 0.6	76.7 ± 0.4
PL QY [%]	57 ± 3	47 ± 3	42 ± 3	41 ± 3
Ligands per SC NC	173 ± 17	154 ± 15	402 ± 40	337 ± 34

19086 | Phys. Chem. Chem. Phys., 2016, 18, 19083–19092

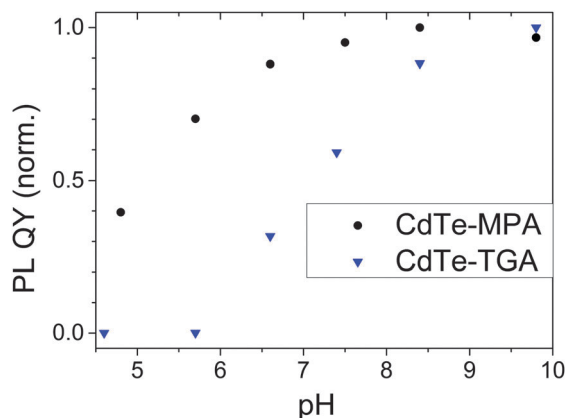This journal is © the Owner Societies 2016

Fig. 3 pH dependence of PL QY of TGA- and MPA-stabilized CdTe T2 and M2 in water. For comparison, the maximum PL QYs are set to 1. The initial PL QY values are given in Table 1. Excitation was at 500 nm.

until pH 9.8. Although PL QY was not measured at more alkaline pH values, considering the slope of the pH-dependent PL QY in comparison to that of the CdTe-MPA sample (M2) shown in Fig. 3, maximum PL QY can be expected for a pH of about 10.

Our observation of a pH-dependent PL QY agrees well with findings from other groups which observed a similar behavior for CdSe and CdTe NCs stabilized with MPA and other thiolate ligands. For example, Gao *et al.* observed a higher PL QY at higher, *i.e.*, alkaline pH for TGA-stabilized CdTe,[48] and Zhang *et al.* demonstrated an improved stability of MPA-capped SC NCs at decreasing pH compared to a TGA surface modification.[49] In a recent study of TGA- and MPA-stabilized CdHgTe colloids, we also found a decrease in PL QY with decreasing pH for TGA- and MPA-capped CdHgTe SC NCs. For these materials, the PL changes are more pronounced for TGA,[14] yet the observed effects were still smaller than the changes occurring for our TGA- and MPA-stabilized CdTe of closely matching size. This underlines the influence of the strength of the ligand–surface atom bond on such dependencies, as the strength of the Hg^{2+}–thiol bond exceeds that of the Cd^{2+}–thiol bond. We ascribe the pH dependence of the PL properties of our TGA- and MPA-functionalized CdTe colloids to a combination of effects, with main contributions arising from the pK_a values of the thiol and carboxylic acid groups of the stabilizing ligands and the onset of particle aggregation and in this respect, also from the ligand shell and the overall number of ligands present in solution. With a pK_a of 3.6, the carboxylic group of the TGA ligand is slightly more acidic than the carboxylic group of MPA (pK_a of 4.32). The pK_a of the thiol groups of TGA and MPA shows the same picture with values of 10.56 and 10.84, respectively.[50] The improved colloidal stability of the MPA-functionalized particles compared to TGA-capped CdTe is most likely related to the *ca.* twofold higher ligand density of the MPA-functionalized SC NCs as revealed by the results of the Ellman's test (see also dilution studies in the next section). Obviously, MPA provides a better stabilization at lower pH values and is more favorable for the preservation of PL at lower pH values than TGA. Moreover, our results underline the importance of ligand analysis.

Influence of SC NC concentration on PL QY in H_2O and D_2O

Dilution studies of the TGA- and MPA-stabilized CdTe colloids in H_2O and D_2O solutions at a constant pH of 9.0 shown in Fig. 4 revealed a decrease of PL QY for both thiol ligands in H_2O for absorbances < 0.01 (concentrations below 2×10^{-7} M). TGA-stabilized colloid T2 seems to be slightly more prone to dilution-induced fluorescence quenching than MPA-capped CdTe NCs M2. A similar reduction in PL QY was previously observed by us for other TGA-stabilized CdTe colloids, with quenching effects depending on SC NC size and hence, surface-to-volume ratio, and on the thickness and morphology of the ligand shell.[8] In contrast, dilution with D_2O at a pD value of 9.0 did not affect the PL QY within our measurement uncertainty of 5%. Moreover, with values of 60% (T2) and 45% (M2), the PL QYs of both colloids in D_2O were slightly higher compared to water. In the literature on II–VI and IV–VI SC NCs, there are various, sometimes even contradictory reports on the quenching and enhancement of the PL of CdSe, CdSe/ZnS, CdTe, and PbS stabilized with different capping agents in different environments and in the presence of various additives.[10,51–55] For example, the emission spectra, PL QY, and PL lifetimes of CdSe/ZnS NCs can be affected by the presence of water molecules (humidity), oxygen (as electron acceptor and by energy transfer), and by other electron donors and acceptors. Common explanations for such effects include the passivation of surface states, photoinduced or chemically induced surface transformation or the rearrangement of capping agents on SC NC surfaces, neutralization of local charged centers inside and outside of SC NCs, photoionization and charge transfer between SC NCs and surface ligands. For example, static quenching of the luminescence of CdSe/ZnS SC NCs, stabilized with a mixture of trioctylphosphine oxide, 4-hexadecylamine, and 11-mercaptoundecanoic acid by differently substituted thiol ligands has been reported, with the extent of the PL diminution depending on the size and charge of the water soluble thiol.[56] Here, PL quenching was mainly ascribed to charge transfer between the SC NCs and the thiols. Although there exist only very few studies comparing H_2O and D_2O, differences in the influence on PL between both solvents have been reported for *e.g.*, CdSe/ZnS
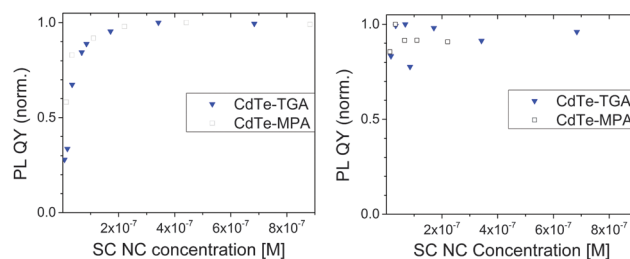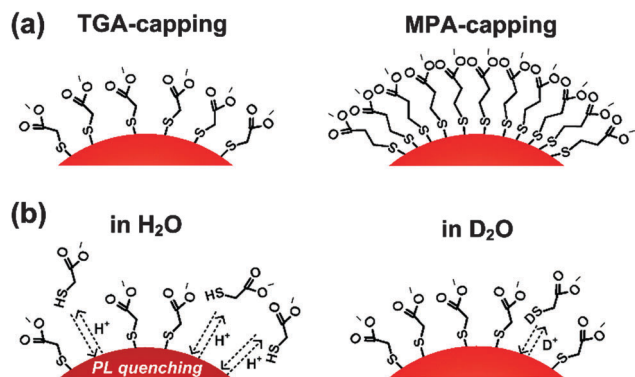

Fig. 4 Left: Normalized PL QYs of TGA- and MPA-stabilized CdTe colloids (T2; M2) in H_2O (pH 9.0) as a function of SC NC concentration. The highest PL QY was set to 1. The initial PL QY values are given in Table 1. Excitation was at 500 nm. Right: Normalized PL QYs of TGA- and MPA-stabilized CdTe colloids (T2; M2) in D_2O (pD 9.4) as a function of SC NC concentration. The highest PL QY was set to 1. The initial PL QY values in D_2O are 60% (T2) and 45% (M2), respectively. Excitation was at 500 nm.

Scheme 1 (a) Schematic presentation of the surface of TGA-capped (left) and MPA-capped (right) CdTe NCs; (b) schematic presentation of the influence of solvent molecules on the surface of TGA-capped CdTe NCs dispersed in H_2O (left) and in D_2O (right). These schematic presentations are not intended to show the actual angle between the CdTe surface and the thiol ligand.

NC colloids, which were attributed to water solvation and stabilization of a charged surface state.[51] We ascribe our findings to two effects or their combination as highlighted in Scheme 1: a shift of the ligand adsorption–desorption equilibrium to the adsorption side, *i.e.*, to the surface-coordinated thiol ligands, by D_2O compared to H_2O and/or the quenching of the fluorescence of SC NCs with partly removed surface ligands by H_2O molecules.

Our findings of a different influence of H_2O and D_2O on the PL properties of TGA- and MPA-stabilized CdTe encouraged us to perform MD simulations of both solvents for studying their hydrogen bond network. As described in the ESI,† these simulations revealed further differences. Apparently, D_2O exhibits 25% less deuterium-bond changes during a simulation time of 30 ps than hydrogen-bond changes occurring in H_2O. This correlates with a slightly longer deuterium-bond lifetime. Both effects are caused by the mass differences between deuterium and hydrogen. This affects the vibrational frequencies of both solvents as well, a fact, which is often utilized to identify water-related quenching of the luminescence of molecular and nano-scale lanthanide emitters.[57,58] The fact that the deuterium-bond network is longer lasting enables different interactions with the ligands at the SC NC surface, which is reflected by different PL QYs. This suggests that a longer-lasting deuterium-bond can favor a more compact ligand shell and hence, a better passivation of surface defects.

Combined precipitation and dilution studies

For a better understanding of the dilution studies and to demonstrate the influence of dilution on the adsorption/desorption equilibrium and on the optical properties, exemplarily precipitation and dilution experiments were performed. In a first step, the amount of ligands required for SC NC stabilization was assessed. For this purpose, we representatively precipitated as synthesized CdTe-MPA colloid M3 by addition of EtOH, separated the SC NCs from excess ligand in solution by decantation and determined the amount of ligand in the filtrate and bound to the still redispersible colloid by ICP-OES. Our results revealed that in

the case of M3, half of the amount of MPA initially applied for SC NC synthesis remained in the filtrate, *i.e.*, in solution. Upon a second washing step, 13% of the remaining ligand shell was removed from the particles, which were nevertheless still redispersible and colloidally stable. More than three precipitation and redispersion steps (PRSs) could not be realized.

Subsequently, we performed dilution studies with TGA- and MPA-stabilized CdTe samples T3 and M3 and assessed the spectroscopic properties of these SC NCs after repeated precipitation with EtOH and subsequent redispersion in H_2O and D_2O. Fig. 5 compares the spectral changes in absorption and emission resulting for TGA-capped samples after successive cycles of precipitation and redispersion (PRS; PRS 1–3) in H_2O (upper panel) and D_2O (lower panel). As follows from this figure, the changes in the emission of TGA-stabilized CdTe are solvent dependent. In H_2O, the emission band shifts to the red with each PRS cycle. In contrast, in D_2O, the spectral position of the PL of TGA-capped CdTe does not change by successive PRS after the first precipitation from the aqueous stock solution of the as synthesized SC NCs. The corresponding absorption
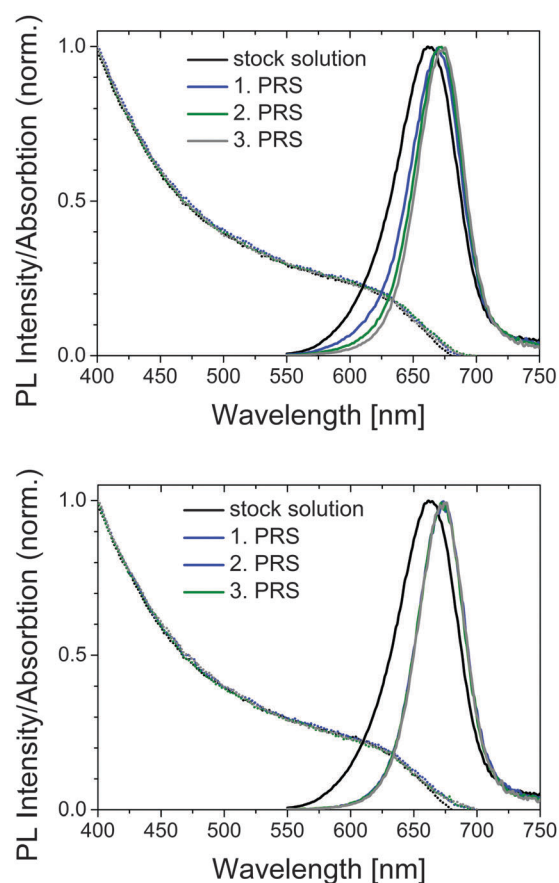

Fig. 5 Normalized absorption (dotted lines) and emission spectra (solid lines) of TGA-capped CdTe in H_2O (upper panel) and D_2O (lower panel) after different precipitation–redispersion steps (PRS; PRS 1–3). Excitation was at 480 nm. The stock solution is the as-synthesized colloid. Absorbances of 0.024 at λ_{ex} were used in both cases equaling a particle concentration of 2.2×10^{-7} M. The absorption spectra shown present the wavelength dependence of the measured absorbance.

19088 | *Phys. Chem. Chem. Phys.*, 2016, **18**, 19083–19092

This journal is © the Owner Societies 2016

spectra of TGA-capped CdTe in H_2O and D_2O are barely affected by successive PRS. The scattering, indicated by an increase in absorbance in the wavelength region of its onset, observed for both samples after three PRS (data not shown), which is accompanied by a slight red shift of the absorption onset, provides hints for Ostwald ripening, particle aggregation, and decrease in colloidal stability. In contrast, in the case of MPA-capped CdTe (data not shown), the absorption spectra and the spectral position of the emission maximum are not affected by the increasing number of PRSs in H_2O and D_2O. This underlines the beneficial impact of MPA stabilization and the influence of the solvent, *i.e.*, its hydrogen bond network.

Subsequently, we performed dilution studies with our TGA- and MPA-stabilized CdTe colloids after each precipitation step, thereby varying the absorbance at the excitation wavelength between 0.01 and 0.10 and hence, the particle concentration in the range of 1×10^{-6} to 1×10^{-7} M. The changes in emission and PL QY resulting for both colloids are summarized in Fig. 6 (inset: emission spectra; H_2O: blue symbols and curves; D_2O: black symbols and curves) for an exemplarily chosen absorbance of 0.024 equaling a particle concentration of 2.2×10^{-7} M and shown in the ESI† (see Fig. S2) for different particle concentrations and PRSs. As follows from Fig. S2 (ESI†), the PL QY is independent of the particle concentration in the range of 1×10^{-6} to 1×10^{-7} M for each precipitation step. As shown in Fig. 6 and Fig. S2 (ESI†) (right panel), the PL QY of the TGA-stabilized CdTe sample decreased with each PRS in both solvents whereas the PL QY of the MPA-capped CdTe colloid (ESI,† Fig. S2, left panel) remained constant even after three PRSs in H_2O and in D_2O in the chosen absorbance/concentration range. Moreover, the emission spectra of TGA-stabilized CdTe shifted to the red (Fig. 6, inset), thereby reflecting the behavior shown in Fig. 5 (upper panel). In contrast, the emission of MPA-capped CdTe did not change its spectral position upon dilution (see Fig. 6, inset, lower panel, and also Fig. 5, lower panel). We ascribe the diminution in PL QY resulting for TGA-capped CdTe to the increasing loss of surface ligands accompanying each PRS, which favors the nonradiative recombination of charge carriers. The fact that the PL QY of MPA-stabilized CdTe is barely affected by up to three PRSs is attributed to the denser initial surface coverage provided by MPA, exceeding that of TGA by a factor of about 2, possibly in conjunction with a higher binding constant of this thiol to the CdTe surface atoms.

In order to assess the influence of pH/pD on such dilution studies, we subsequently performed dilution cycles solely with the more stable MPA-capped CdTe M3 at acidic pD in D_2O (pD 6.4) and recorded PL decay curves. The lifetimes calculated from these decay curves, which are summarized in Fig. 7 (inset), represent the time after which the initial fluorescence intensity decreased to the $1/e$ part of its maximum value. Although the luminescence decay curves of SC NC are occasionally fitted with a double exponential fit, with the resulting decay components being assigned *e.g.*, to the recombination of core states and radiative carrier recombination associated with the involvement of surface states,[59,60] we favor here this simple, yet in our opinion more physically meaningful model for SC NC with a distribution of sizes and surface states. An analysis of the lifetime data with stretched exponential fits, yielding decay rate probability functions, as suggested by some authors to obtain a more descriptive picture of the results from time-resolved PL studies with SC NC,[61–63] is shown in the ESI.† In addition to time-resolved PL measurements, the PL QY was determined as previously described.

As follows from Fig. 7, at acidic pD values, also the PL QY and the PL lifetime of CdTe-MPA becomes concentration-dependent, with a diminution in fluorescence resulting for particle concentrations $< 5 \times 10^{-7}$ M. A strong change in fluorescence intensity accompanied by an unchanged or barely influenced fluorescence lifetime provides a hint for an inhomogeneous quenching (some emitters are quenched while others remain unaffected) whereas a diminution of the fluorescence quantum yield accompanied by a reduction in emission lifetime as observed here presents an indicator for homogeneous quenching, with all emitters being similarly affected.[64]
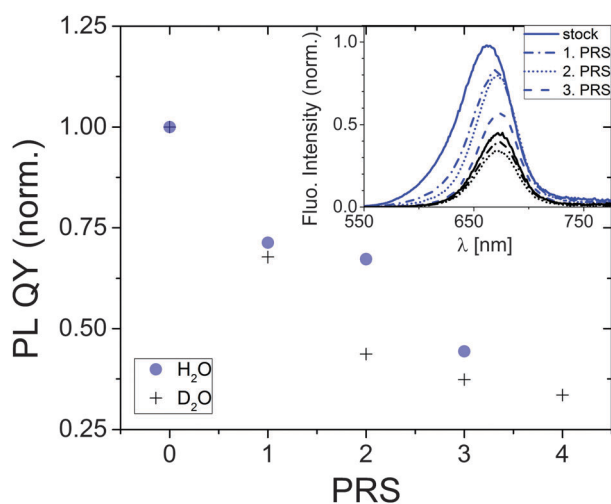

Fig. 6   PL QY of TGA-stabilized CdTe samples as a function of precipitation steps with EtOH and redispersion in H_2O (blue) or D_2O (black). The samples were excited at 480 nm and their absorbance at λ_{ex} was held constant at 0.024 equaling a particle concentration of 2.2×10^{-7} M. The inset shows the corresponding emission spectra.
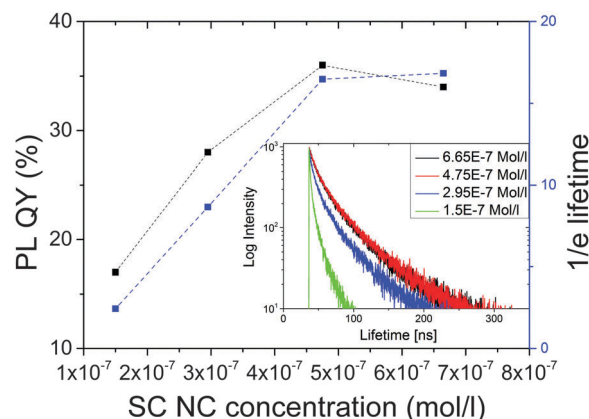

Fig. 7   PL QY and $1/e$ fluorescence lifetime of CdTe-MPA sample M3 upon dilution in D_2O at pD 6.4. Inset: Corresponding decay curves. Excitation was at 500 nm. The dashed line presents a guide for the eye only.

Conclusion and outlook

In summary, the influence of pH, particle concentration, and redispersion-dilution cycles on the colloidal stability and photoluminescence properties of a set of analytically well characterized CdTe colloids stabilized with the monodentate thiols TGA and MPA were systematically assessed in water and D_2O using steady state and time-resolved fluorometry. Our results clearly demonstrate ligand control of the pH-dependence, of the colloidal stability and PL behavior, *i.e.*, the extent of the pH-related spectral shifts in emission and fluorescence quenching. Moreover, we stress the importance of hydrogen bonding and the stability of the thiol–surface atom bond for the PL properties of ligand-capped SC NCs. MPA-stabilized CdTe colloids revealed an improved stability and a reduced sensitivity to luminescence quenching. The pH dependence of the PL properties of our TGA- and MPA-functionalized CdTe colloids is controlled by different parameters including the pK_a values of the thiol and carboxylic acid groups of the capping ligands, the ligand shell itself, and the overall number of ligands present in solution from particle synthesis. This highlights the importance of ligand analysis necessary for the knowledge of the overall ligand concentration and the number of ligands per SC NC for SC NC stability control and optimum PL properties.

Our findings provide straightforward tools to compare the quality and performance of CdTe SC NCs functionalized with small monodentate thiol ligands like TGA and MPA, which are the most commonly used stabilizing ligands for these SC NC. Our approach can be most likely transferred to other SC NC and ligand systems in the future. This can be beneficial for the design of SC NCs with improved PL properties. In this respect, we will assess also the size dependence of these effects and perform similar studies with CdTe NCs stabilized with other thiols.

Abbreviations

pH	Negative logarithm of acid concentration
pD	pH equivalent for deuterated solutions
SC	Semiconductor
NC	Nanocrystal
TGA	Thioglycolic acid
MPA	Mercaptopropionic acid
PL	Photoluminescence
QY	Quantum yield
HOMO	Highest occupied molecular orbital
LUMO	Lowest unoccupied molecular orbital
TG	1-Thioglycerol
MA	Amine-terminated 1-thioglycerol
NMR	Nuclear magnetic resonance
DTNB	5,5′-Dithiobis(2-nitrobenzoic acid)
EDTA	Ethylenediaminetetraacetic acid
TEM	Transmission electron microscopy
T	Temperature
TCSPC	Time-correlated single-photon counting
ICP-OES	Inductively coupled plasma-optical emission spectroscopy
MD	Molecular dynamics
PRS	Precipitation step
ex	Excitation
em	Emission

Author contributions

The manuscript was written through contributions of all authors. All authors have given approval to the final version of the manuscript.

Acknowledgements

References

1 D. V. Talapin, J. S. Lee, M. V. Kovalenko and E. V. Shevchenko, *Chem. Rev.*, 2010, **110**, 389.

2 Y. C. Wang, R. Hu, G. M. Lin, I. Roy and K. T. Yong, *ACS Appl. Mater. Interfaces*, 2013, **5**, 2786–2799.

3 M. V. Kovalenko, L. Manna, A. Cabot, Z. Hens, D. V. Talapin, C. R. Kagan, V. I. Klimov, A. L. Rogach, P. Reiss, D. J. Milliron, P. Guyot-Sionnnest, G. Konstantatos, W. J. Parak, T. Hyeon, B. A. Korgel, C. B. Murray and W. Heiss, *ACS Nano*, 2015, **9**, 1012–1057.

4 D. A. Hines and P. V. Kamat, *ACS Appl. Mater. Interfaces*, 2014, **6**, 3041–3057.

5 M. D. Peterson, L. C. Cass, R. D. Harris, K. Edme, K. Sung and E. A. Weiss, in *Annu. Rev. Phys. Chem.*, ed. M. A. Johnson and T. J. Martinez, 2014, vol. 65, pp. 317–339.

6 A. M. Munro, I. J. L. Plante, M. S. Ng and D. S. Ginger, *J. Phys. Chem. C*, 2007, **111**, 6220–6227.

7 M. D. Garrett, A. D. Dukes, J. R. McBride, N. J. Smith, S. J. Pennycook and S. J. Rosenthal, *J. Phys. Chem. C*, 2008, **112**, 12736–12746.

8 M. Grabolle, M. Spieles, V. Lesnyak, N. Gaponik, A. Eychmüller and U. Resch-Genger, *Anal. Chem.*, 2009, **81**, 6285–6294.

9 K. E. Knowles, M. T. Frederick, D. B. Tice, A. J. Morris-Cohen and E. A. Weiss, *J. Phys. Chem. Lett.*, 2012, **3**, 18–26.

10 J. Aldana, Y. A. Wang and X. Peng, *J. Am. Chem. Soc.*, 2001, **123**, 8844–8850.

11 A. J. Morris-Cohen, M. Malicki, M. D. Peterson, J. W. J. Slavin and E. A. Weiss, *Chem. Mater.*, 2013, **25**, 1155–1165.

12 A. Mandal and N. Tamai, *Appl. Phys. Lett.*, 2011, **99**, 263111.

13 Y. Shen, R. Tan, M. Y. Gee and A. B. Greytak, *ACS Nano*, 2015, **9**, 3345–3359.

14 S. Leubner, R. Schneider, A. Dubavik, S. Hatami, N. Gaponik, U. Resch-Genger and A. Eychmüller, *J. Mater. Chem. C*, 2014, **2**, 5011–5018.

15 S. Leubner, S. Hatami, N. Esendemir, T. Lorenz, J. O. Joswig, V. Lesnyak, S. Recknagel, N. Gaponik, U. Resch-Genger and A. Eychmüller, *Dalton Trans.*, 2013, **42**, 12733–12740.

16 J. Ziegler, A. Merkulov, M. Grabolle, U. Resch-Genger and T. Nann, *Langmuir*, 2007, **23**, 7751–7759.

17 S. H. Xu, C. L. Wang, Z. Y. Wang, H. S. Zhang, J. Yang, Q. Y. Xu, H. B. Shao, R. Q. Li, W. Lei and Y. P. Cui, *Nanotechnology*, 2011, **22**, 275605.

18 J. Park, J. Nam, N. Won, H. Jin, S. Jung, S. Jung, S. H. Cho and S. Kim, *Adv. Funct. Mater.*, 2011, **21**, 1558–1566.

19 N. Zhan, G. Palui, A. Kapur, V. Palomo, P. E. Dawson and H. Mattoussi, *J. Am. Chem. Soc.*, 2015, **137**, 16084–16097.

20 N. Q. Zhan, G. Palui and H. Mattoussi, *Nat. Protoc.*, 2015, **10**, 859–874.

21 G. Palui, F. Aldeek, W. T. Wang and H. Mattoussi, *Chem. Soc. Rev.*, 2015, **44**, 193–227.

22 V. Lesnyak, N. Gaponik and A. Eychmüller, *Chem. Soc. Rev.*, 2013, **42**, 2905–2929.

23 A. L. Rogach, T. Franzl, T. A. Klar, J. Feldmann, N. Gaponik, V. Lesnyak, A. Shavel, A. Eychmüller, Y. P. Rakovich and J. F. Donegan, *J. Phys. Chem. C*, 2007, **111**, 14628–14637.

24 N. Gaponik, D. V. Talapin, A. L. Rogach, K. Hoppe, E. V. Shevchenko, A. Kornowski, A. Eychmüller and H. Weller, *J. Phys. Chem. B*, 2002, **106**, 7177–7185.

25 I. Moreels, J. C. Martins and Z. Hens, *Sens. Actuators, B*, 2007, **126**, 283–288.

26 I. Moreels, B. Fritzinger, J. C. Martins and Z. Hens, *J. Am. Chem. Soc.*, 2008, **130**, 15081–15086.

27 B. Fritzinger, I. Moreels, P. Lommens, R. Koole, Z. Hens and J. C. Martins, *J. Am. Chem. Soc.*, 2009, **131**, 3024–3032.

28 A. Hassinen, I. Moreels, C. de Mello Donegá, J. C. Martins and Z. Hens, *J. Phys. Chem. Lett.*, 2010, **1**, 2577–2581.

29 B. Fritzinger, R. K. Capek, K. Lambert, J. C. Martins and Z. Hens, *J. Am. Chem. Soc.*, 2010, **132**, 10195–10201.

30 R. Gomes, A. Hassinen, A. Szczygiel, Q. Zhao, A. Vantomme, J. C. Martins and Z. Hens, *J. Phys. Chem. Lett.*, 2011, **2**, 145–152.

31 W. W. Yu, L. H. Qu, W. Z. Guo and X. G. Peng, *Chem. Mater.*, 2003, **15**, 2854–2860.

32 X. Ji, D. Copenhaver, C. Sichmeller and X. Peng, *J. Am. Chem. Soc.*, 2008, **130**, 5726–5735.

33 K. D. Mielenz, E. D. Cehelnik and R. L. McKenzie, *J. Chem. Phys.*, 1976, **64**, 370–374.

34 C. Würth, M. Grabolle, J. Pauli, M. Spieles and U. Resch-Genger, *Nat. Protoc.*, 2013, **8**, 1535–1550.

35 C. Würth, D. Geißler and U. Resch-Genger, *Z. Phys. Chem.*, 2015, **229**, 153–165.

36 U. Resch-Genger and P. C. DeRose, *Pure Appl. Chem.*, 2012, **84**, 1815–1835.

37 T. Felbeck, T. Behnke, K. Hoffmann, M. Grabolle, M. M. Lezhnina, U. H. Kynast and U. Resch-Genger, *Langmuir*, 2013, **29**, 11489–11497.

38 G. L. Ellman, *Arch. Biochem. Biophys.*, 1959, **82**, 70–77.

39 M. Moser, T. Behnke, C. Hamers-Allin, K. Klein-Hartwig, J. Falkenhagen and U. Resch-Genger, *Anal. Chem.*, 2015, **87**, 9376–9383.

40 P. K. Glasoe and F. A. Long, *J. Phys. Chem.*, 1960, **64**, 188–190.

41 D. Porezag, T. Frauenheim, T. Köhler, G. Seifert and R. Kaschner, *Phys. Rev. B: Condens. Matter Mater. Phys.*, 1995, **51**, 12947–12957.

42 G. Seifert, D. Porezag and T. Frauenheim, *Int. J. Quantum Chem.*, 1996, **58**, 185–192.

43 G. Seifert and J.-O. Joswig, *Wiley Interdiscip. Rev.: Comput. Mol. Sci.*, 2012, **2**, 456–465.

44 M. Elstner, D. Porezag, G. Jungnickel, J. Elsner, M. Haugk, T. Frauenheim, S. Suhai and G. Seifert, *Phys. Rev. B: Condens. Matter Mater. Phys.*, 1998, **58**, 7260–7268.

45 J. O. Joswig and G. Seifert, *J. Phys. Chem. B*, 2009, **113**, 8475–8480.

46 W. L. Cavalcanti, D. F. Portaluppi and J. O. Joswig, *J. Chem. Phys.*, 2010, **133**, 104703.

47 Y. Zhang, J. He, P.-N. Wang, J.-Y. Chen, Z.-J. Lu, D.-R. Lu, J. Guo, C.-C. Wang and W.-L. Yang, *J. Am. Chem. Soc.*, 2006, **128**, 13396–13401.

48 M. Gao, S. Kirstein, H. Möhwald, A. L. Rogach, A. Kornowski, A. Eychmüller and H. Weller, *J. Phys. Chem. B*, 1998, **102**, 8360–8363.

49 H. Zhang, Z. Zhou, B. Yang and M. Gao, *J. Phys. Chem. B*, 2003, **107**, 8–13.

50 S. Xu, C. Wang, H. Zhang, Z. Wang, B. Yang and Y. Cui, *Nanotechnology*, 2011, **22**, 315703.

51 K. Pechstedt, T. Whittle, J. Baumberg and T. Melvin, *J. Phys. Chem. C*, 2010, **114**, 12069–12077.

52 J. Muller, J. M. Lupton, A. L. Rogach, J. Feldmann, D. V. Talapin and H. Weller, *Appl. Phys. Lett.*, 2004, **85**, 381–383.

53 A. C. S. Samia, X. Chen and C. Burda, *J. Am. Chem. Soc.*, 2003, **125**, 15736–15737.

54 S. W. Buckner, R. L. Konold and P. A. Jelliss, *Chem. Phys. Lett.*, 2004, **394**, 400–404.

55 S. Hatami, C. Wurth, M. Kaiser, S. Leubner, S. Gabriel, L. Bahrig, V. Lesnyak, J. Pauli, N. Gaponik, A. Eychmüller and U. Resch-Genger, *Nanoscale*, 2015, **7**, 133–143.

56 V. V. Breus, C. D. Heyes and G. U. Nienhaus, *J. Phys. Chem. C*, 2007, **111**, 18589–18594.

57 S. Wilhelm, M. Kaiser, C. Wurth, J. Heiland, C. Carrillo-Carrion, V. Muhr, O. S. Wolfbeis, W. J. Parak, U. Resch-Genger and T. Hirsch, *Nanoscale*, 2015, **7**, 1403–1410.

58 R. Arppe, I. Hyppanen, N. Perala, R. Peltomaa, M. Kaiser, C. Wurth, S. Christ, U. Resch-Genger, M. Schaferling and T. Soukka, *Nanoscale*, 2015, **7**, 11746–11757.

This journal is © the Owner Societies 2016

Phys. Chem. Chem. Phys., 2016, **18**, 19083–19092 | **19091**

59 K. Zhao, J. Li, H. Wang, J. Zhuang and W. Yang, *J. Phys. Chem. C*, 2007, **111**, 5618–5621.

60 S. J. Byrne, S. A. Corr, T. Y. Rakovich, Y. K. Gun'ko, Y. P. Rakovich, J. F. Donegan, S. Mitchell and Y. Volkov, *J. Mater. Chem.*, 2006, **16**, 2896–2902.

61 G. Zatryb, A. Podhorodecki, J. Misiewicz, J. Cardin and F. Gourbilleau, *Nanoscale Res. Lett.*, 2011, **6**, 106.

62 A. Van Driel, I. Nikolaev, P. Vergeer, P. Lodahl, D. Vanmaekelbergh and W. Vos, *Phys. Rev. B: Condens. Matter Mater. Phys.*, 2007, **75**, 035329.

63 R. Saito and K. Murayama, *Solid State Commun.*, 1987, **63**, 625–627.

64 N. C. Bigall, W. J. Parak and D. Dorfs, *Nano Today*, 2012, 7, 282–296.

19092 | *Phys. Chem. Chem. Phys.*, 2016, **18**, 19083–19092

This journal is © the Owner Societies 2016